

OncoImmunology

ISSN: 2162-402X (Online) Journal homepage: www.tandfonline.com/journals/koni20

An integral membrane constitutively active heparanase enhances the tumor infiltration capability of NK cells

Sofia Liborio-Ramos, Isaac Quiros-Fernandez, Neta Ilan, Soaad Soboh, Malik Farhoud, Ruken Süleymanoglu, Michele Bennek, Sara Calleja-Vara, Martin Müller, Israel Vlodavsky & Angel Cid-Arregui

To cite this article: Sofia Liborio-Ramos, Isaac Quiros-Fernandez, Neta Ilan, Soaad Soboh, Malik Farhoud, Ruken Süleymanoglu, Michele Bennek, Sara Calleja-Vara, Martin Müller, Israel Vlodavsky & Angel Cid-Arregui (2025) An integral membrane constitutively active heparanase enhances the tumor infiltration capability of NK cells, OncoImmunology, 14:1, 2437917, DOI: 10.1080/2162402X.2024.2437917

To link to this article: https://doi.org/10.1080/2162402X.2024.2437917

© 2024 The Author(s). Published with license by Taylor & Francis Group, LLC.

View supplementary material

Published online: 09 Dec 2024.

Submit your article to this journal

Article views: 3055

View related articles

View Crossmark data

Citing articles: 5 View citing articles

Full Terms & Conditions of access and use can be found at
https://www.tandfonline.com/action/journalInformation?journalCode=koni20

ONCOIMMUNOLOGY
2025, VOL. 14, NO. 1, 2437917
https://doi.org/10.1080/2162402X.2024.2437917

Taylor & Francis
Taylor & Francis Group

ORIGINAL RESEARCH

OPEN ACCESS Check for updates

An integral membrane constitutively active heparanase enhances the tumor infiltration capability of NK cells

Sofia Liborio-Ramos[a*], Isaac Quiros-Fernandez[a,b*], Neta Ilan[c], Soaad Soboh[c], Malik Farhoud[c], Ruken Süleymanoglu[a], Michele Bennek[a], Sara Calleja-Vara[a], Martin Müller[d], Israel Vlodavsky[c], and Angel Cid-Arregui[a]

[a]Targeted Tumor Vaccines Group, Clinical Cooperation Unit Applied Tumor Immunity, German Cancer Research Center (DKFZ), Heidelberg, Germany; [b]Research Center on Tropical Diseases (CIET)/Research Center on Surgery and Cancer (CICICA), Faculty of Microbiology, Universidad de Costa Rica, San Jose, Costa Rica; [c]Technion Integrated Cancer Center (TICC), Rappaport Faculty of Medicine, Technion - Israel Institute of Technology, Haifa, Israel; [d]Tumorvirus-specific Vaccination Strategies, German Cancer Research Center (DKFZ), Heidelberg, Germany

ABSTRACT

Eradication of cancer cells by the immune system requires extravasation, infiltration and progression of immune cells through the tumor extracellular matrix (ECM). These are also critical determinants for successful adoptive cell immunotherapy of solid tumors. Together with structural proteins, such as collagens and fibronectin, heparan sulfate (HS) proteoglycans are major components of the ECM. Heparanase 1 (HPSE) is the only enzyme known to have endoglycosidase activity that degrades HS. HPSE is expressed at high levels in almost all hematopoietic cells, which suggests that it plays a relevant role in immune cell migration through solid tissues. Besides, tumor cells express also HPSE as a way to facilitate tumor cell resettlement and metastasis. Therefore, an increase in HPSE in the tumor ECM would be detrimental. Here, we analyzed the effects of constitutive expression of an active, membrane-bound HPSE on the ability of human natural killer (NK) cells to infiltrate tumors and eliminate tumor cells. We demonstrate that NK cells expressing a chimeric active form of HPSE on the cell surface as an integral membrane protein, display significantly enhanced infiltration capability into spheroids of various cancer cell lines, as well as into xenograft tumors in immunodeficient mice. As a result, tumor growth was significantly suppressed without causing noticeable side effects. Altogether, our results suggest that a constitutively expressed active HSPE on the surface of immune effector cells enhances their capability to access and eliminate tumor cells. This strategy opens new possibilities for improving adoptive immune treatments using NK cells.

ARTICLE HISTORY
Received 22 October 2024
Revised 28 November 2024
Accepted 29 November 2024

KEYWORDS
Adoptive cell transfer; CAR; cell therapy; chimeric antigen receptor; heparanase; immunotherapy; natural killer (NK) cells; T cell receptor

Introduction

Natural killer (NK) and T cells engineered to express either a chimeric antigen receptor (CAR) or a transgenic T cell receptor (TCR) reactive to tumor antigens are the basis of adoptive cell therapy (ACT), which has shown remarkable clinical responses in B cell malignancies. Indeed, a number of CAR-based strategies are currently being tested in clinical trials.[1] However, to date only one ACT therapy for solid tumors has reached the clinic: a TCR targeting MAGE-A4, which has been authorized very recently for metastatic synovial sarcoma.[2] In contrast to hematological cancers, solid tumors are more complex and well-organized tissue structures comprising tumor cells and a mixture of supporting cells, immune cells and vessels immersed in extracellular matrix (ECM), altogether representing the tumor microenvironment.[3] In general, high numbers of immune cells in a tumor correlate with longer progression-free survival and overall survival of patients.[4]

NK cells are a subclass of lymphocytes essential for tumor immunosurveillance. They can eliminate cancer cells by releasing cytotoxic products such as perforin and granzymes, and release cytokines that recruit other immune cells to the tumor microenvironment (TME).[3] An essential feature of NK cells is that, unlike T cells, they do not require antigen processing and presentation to recognize their target cells. Moreover, HLA mismatched NK cells can be delivered with no risk of graft vs. host disease (GVHD), which makes them good off-the-shelf candidates for ACT.[5] Yet, infusion of NK cells in patients with solid tumors has not delivered encouraging clinical outcomes. Preclinical and clinical data suggest that their efficacy in solid tumors is limited by inadequate tumor infiltration and migration across the TME.[6]

To fulfill their immunosurveillance function, immune cells infiltrate tissues by first crossing the subendothelial basal membrane and then migrating through the ECM. Infiltration of tumor tissues by NK and T cells after extravasation requires controlled local degradation of the ECM, composed by structural proteins (collagens, laminin, fibronectin, vitronectin), cleaved by matrix metalloproteinases, and heparan sulfate (HS) proteoglycans

CONTACT Angel Cid-Arregui a.cid@dkfz-heidelberg.de Targeted Tumor Vaccines Group, Applied Tumor Immunity, German Cancer Research Center (DKFZ), Im Neuenheimer Feld 280, Heidelberg 69120, Germany

*Both authors contributed equally.

Supplemental data for this article can be accessed online at https://doi.org/10.1080/2162402X.2024.2437917

© 2024 The Author(s). Published with license by Taylor & Francis Group, LLC.
This is an Open Access article distributed under the terms of the Creative Commons Attribution-NonCommercial License (http://creativecommons.org/licenses/by-nc/4.0/), which permits unrestricted non-commercial use, distribution, and reproduction in any medium, provided the original work is properly cited. The terms on which this article has been published allow the posting of the Accepted Manuscript in a repository by the author(s) or with their consent.

(HSPGs), which are major ECM constituents. Heparanase 1 (HPSE), the only known HS degrading endoglycosidase, and it is widely expressed among immune cells and by tumor cells.[7]

Here, we aimed to provide a new strategy for improved ACT that might address various types of cancer through enhancing the infiltration ability of NK and T cells. We have designed and developed a strategy to enhance the infiltration and mobility of NK cells into solid tumors by incorporating a constitutively active form of HPSE (GS3)[8] as an integral membrane protein on the surface of NK cells (GS3^{TM}). In this study, we show that a derivative of the NK-92 cell line (NK-92$^{CD3/CD8}$/GS3^{TM}) exhibits enhanced infiltration across ECM, tumor spheroids and tumor xenografts. Accordingly, tumor growth was significantly reduced in grafted mice without noticeable side effects. The data suggests that HPSE facilitates the infiltration of activated human NK cells into the tumor sites, opening new possibilities for more efficient immune treatments based on NK and T cell delivery.

Materials and methods

See Supplementary Information

Results

Expression of HPSE in primary NK cells is diminished upon activation

It has been reported previously that CD8+ T cells loose expression of HPSE after culture *ex vivo*.[9] However, very little is known about the expression of HPSE in NK cells under culture conditions. We analyzed the expression profile of HPSE in primary NK cells in PBMCs from healthy donors, maintained *ex vivo* under resting or activating conditions. All NK cells (CD56^{dim} and CD56^{bright}) express HPSE with slightly higher intensities observed in CD56^{bright} cells (Figure 1a). Stimulation of the primary NK cells with irradiated T2 feeder cells induced their proliferation as expected, from 10% to 56% at 2 days and 75% at 10 days of coincubation, with a concomitant transient enhancement of HPSE expression followed by a decay after two weeks in culture independently of the varying frequencies of NK cells along the expansion (Figure 1b). We also tested the expression of HPSE in the human NK92$^{CD3/CD8}$ cell line, a derivative of the NK-92 cell line genetically modified to constitutively express the human CD3 and CD8 proteins, which makes possible the expression and proper assembly on the cell surface of a transgenic TCR complex.[10] Activation of this cell line with PMA and ionomycin induced a transient increase in HPSE expression (Figure 1c) followed by a decay to normal levels (not represented). Furthermore, coincubation of NK92$^{CD3/CD8}$ cells with FaDu and UPCI-SCC-154 cells, both head and neck squamous cell carcinoma cell lines, caused a significant decrease in HPSE expression after 72 hours. Altogether these results suggest that activation of the NK cells leads to a decrease in HPSE expression.

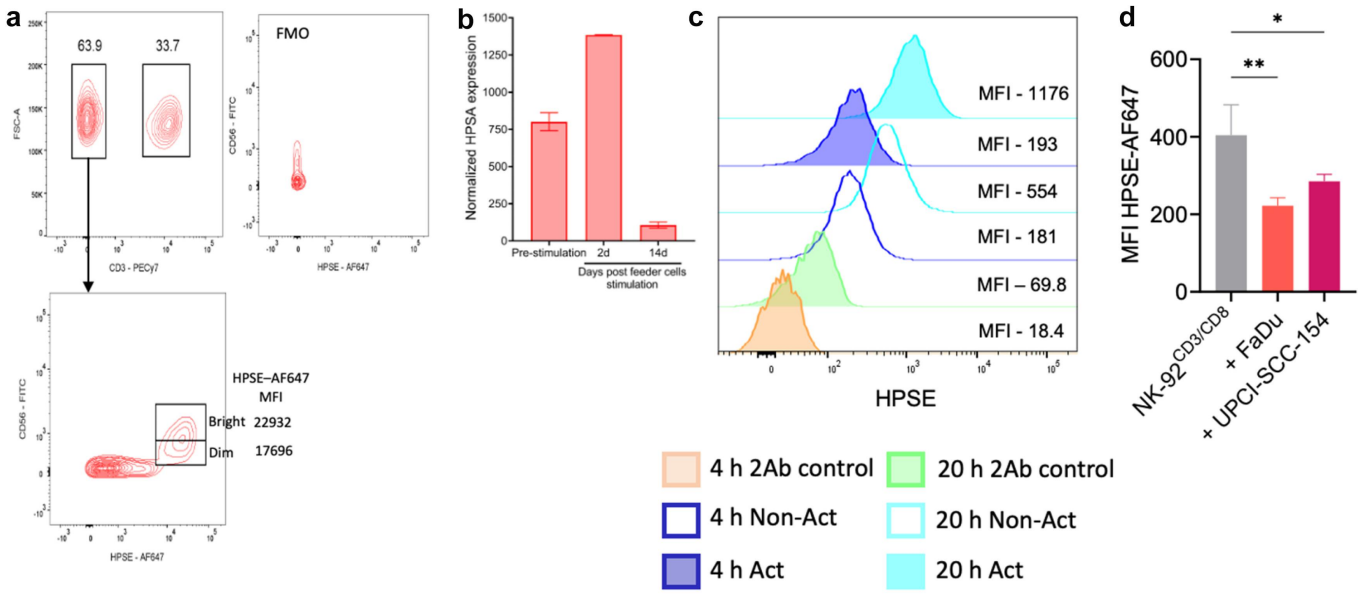


Figure 1. HPSE expression in human NK cells. (a) surface expression of HPSE in primary NK cells of PBMCs from three healthy donors. After isolation, aliquots of PBMCs were retrieved and stained with anti-CD3-PECy7, anti-CD56-fitc and anti-hpse (hpa 733+anti-rabbit-AF647). CD3^{-} cells were gated (upper-left graph) and analyzed for HPSE expression (lower graph). The negative control omitting the anti HPSE (fluorescence-minus-one, FMO) is shown in the upper-right graph. (b) changes in expression of HPSE upon stimulation of PBMCs by co-culture with irradiated T2 feeder cells. As expected, the percentages of NK cells were increasing throughout the coculture. At the indicated time points, the cells were stained with anti-CD3-apc, anti-CD56-pe, anti-hpa 733 (detection with anti-rabbit-AF647) antibodies. Live (DAPI-)/CD56+/CD3- cells were gated and the median fluorescence intensity (MFI) for AF647 (HPSE) was measured. For each time point, a negative control for the HPSE staining was carried out by omitting the primary anti-hpa 733 antibody. The normalized HPSE expression was calculated by dividing the MFI of the AF647 (HPSE) by the MFI of the negative control. (c) effect of a 4-hour activation of NK92$^{CD3/CD8}$ cells with PMA and ionomycin on HPSE expression in NK92 cells. The graphs show the MFI of HPSE detected with anti-hpa 733 and an anti-rabbit secondary antibody conjugated with AF647. (d) decrease in HPSE expression on the surface of NK92$^{CD3/CD8}$ cells cocultured for 72 hours with the indicated HNSCC cell lines. Histograms are normalized to mode. Isotype control (orange), non-activated cells (grey) and activated cells (purple). Results are shown as the mean ± standard deviation (SD). The cells were stained with anti-hpa 733 and CD56 antibodies. Stars * and ** represent p-values <0.05 and <0.01, respectively.

HPSE facilitates the infiltration of mouse NK cells into growing tumor spheroids

To investigate the effects of HPSE on the migration ability of NK cells *in vivo*, we used HPSE knockout (HPSE-KO) mice that were generated earlier.[11] HPSE-KO mice are viable, fertile and develop normally.[12] The absence of an altered phenotype in these mice was attributed to a concomitant overexpression of matrix metalloproteinases.[11] Nevertheless, it was subsequently found that macrophages isolated from HPSE-KO mice express lower levels of cytokines, such as TNFα and IL1-β, and have lower motility and phagocytic activity.[13] Yet, there is little information on the function of HPSE in NK cells. We isolated NK cells from wild type and HPSE-KO mice (Figure 2a) and, after confirming the absence of heparanase activity in HPSE-KO NK cells (Figure 2b), we analyzed their ability to infiltrate spheroids of the TC-1 syngenic tumor cell line established by transfecting lung epithelial cells with a mutant HRAS(G12V) gene and the human papillomavirus type 16 E6 and E7 genes.[14] Confocal microscopy analysis of spheroids co-cultured with the respective NK cells showed profuse and deep infiltration of the spheroids by wild type NK cells. In contrast, NK cells from HPSE-KO mice were significantly lower in number and localized mainly in the margins of the spheroids (Figure 2c,d). These results support the relevant role of HPSE in facilitating NK cell mobility and tumor infiltration.

Expression of active HPSE as an integral membrane protein in NK cells enhances their heparanase enzymatic activity and stimulate cytokine release

HPSE is expressed in all immune cells and is thought to be implicated in the infiltration and migration functions of these cells through inflamed and tumor tissues due to its ECM remodeling activity.[15] A previous study showed that overexpression of HPSE in chimeric antigen receptor (CAR) T lymphocytes enhanced their tumor infiltration ability.[9] Given that HPSE is known to promote tumor invasiveness, angiogenesis,[16] we reasoned that endowing NK cells with an active form of HPSE as an integral membrane protein would facilitate their migration through the tumor ECM, while it would not support tumor cell movement. We first constructed a synthetic fusion gene coding for a chimeric protein composed of an N-terminal extracellular HPSE GS3 linked to a CD28 transmembrane domain and an intracellular mWasabi[17] (supplementary information, fig S1A) cloned in a sleeping beauty system.[18,19] In stably transfected NK-92 $^{CD3/CD8}$ cells we were not able to detect an increase in HPSE on the cell surface, in spite of the construct correctness and the expression of mWasabi being visible (green fluorescence) (supplementary information, fig S1B-F). A plausible explanation is that the mWasabi protein aggregated in an intracellular compartment and, therefore, the fusion protein could not reach the cell surface.

We then decided to remove the mWasabi domain from the previous construct and express a GS3 protein with an

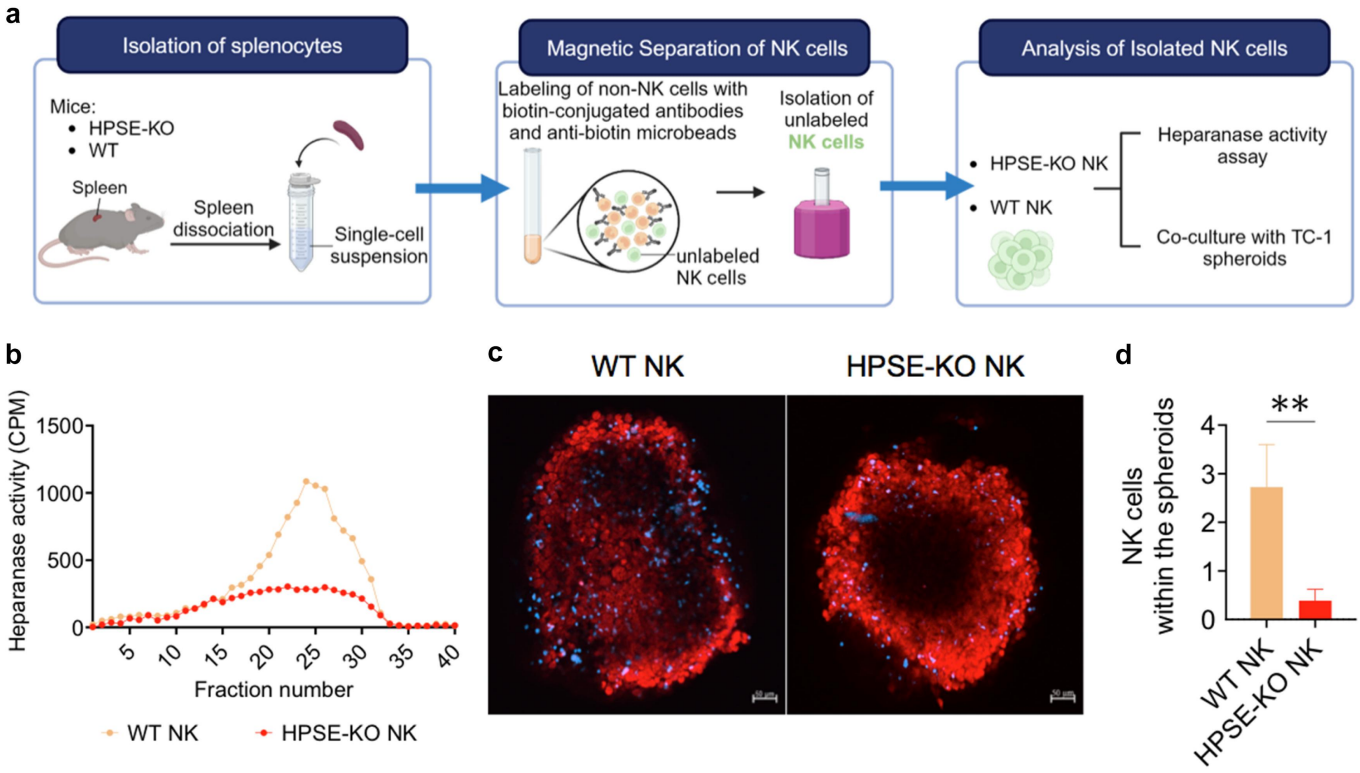


Figure 2. Knock-out of HPSE in mice reduces the infiltration capability of NK cells. (a) flow-chart of the isolation and analysis of NK cells from wild type (WT) and HPSE-KO mice. (b) Heparanase activity in NK cells isolated from either WT or HPSE-KO mice and plated on ^{35}S-sulfate labeled ECM dishes. After 18 h incubation, the labeled HS degradation fragments were quantified in a β-scintillation counter. HPSE-KO NK cells showed little or no heparanase activity above background levels. (c) Representative confocal microscopy image of TC-1 spheroids co-cultured for 24 h with fluorescently labeled NK cells isolated from either HPSE-KO or WT mice. The spheroids (n=5) were fixed, counterstained with propidium iodide and analyzed by confocal microscopy. Images show the merge of blue (NK cells) and red (TC1 cells) fluorescence. The experiment was repeated twice. Scale bar: 50 µm. (d) quantification of infiltrating NK cells within the spheroid area. The percentages of infiltrating NK cells were calculated by the ratio of the integrated violet fluorescence intensities measured per spheroid area. Data are mean percentages of five samples per group ± SD. (**) p-value <0.01.

N-terminal MYC tag and linked at its C-terminus to the CD28 hinge and transmembrane domains (named GS3^{TM}), with no intracellular mWasabi domain (Figure 3a). We detected the presence of the GS3 on the surface of NK92$^{CD3/CD8}$/GS3^{TM} transfected cells with an anti-Myc tag antibody that was used to sort the stably transfected cells (supplementary information, fig. S2). Then we analyzed the expression of GS3 in these cells in three ways: (i) by conventional flow cytometry using anti-Hpa 733 polyclonal antibodies, which detect both endogenous HPSE and transgenic GS3^{TM}. We measured 4-fold higher median fluorescence intensity (MFI) values in NK92$^{CD3/CD8}$/GS3^{TM} cells over non-transfected NK92$^{CD3/CD8}$ cells (Figure 3b); (ii) such difference was also demonstrated by imaging flow cytometry (Figure 3c,d), which additionally showed the distribution of the HPSE and GS3 proteins as patches throughout the cell surface; and (iii) heparanase activity measured in the GS3^{TM} transgenic cells was about 3-fold higher than the activity detected in non-transfected cells (Figure 3e). To examine whether constitutive expression of GS3^{TM} affects the appearance of cellular membrane proteins, we analyzed the expression of CD56 and a panel of lineage-specific NK receptors (Figure 3f). The expression levels of CD56, NKp30, NKG2A and KIR2DL4 were comparable with those of non-transfected cells, A broader receptor profiling did not show significant differences between both cell lines (supplementary information, fig. S2). However, we detected a slight decrease in the levels of NKp44, NKp46 and NKG2D. Interestingly, such small reduction did not affect the ability of the cells to get activated upon co-cultivation with two different HNSCC tumor cell lines (Figure 3g). Indeed, a significantly higher activation of NK92$^{CD3/CD8}$/GS3^{TM} cells co-cultured with FADU compared with UPCI-SCC-154 cells correlated

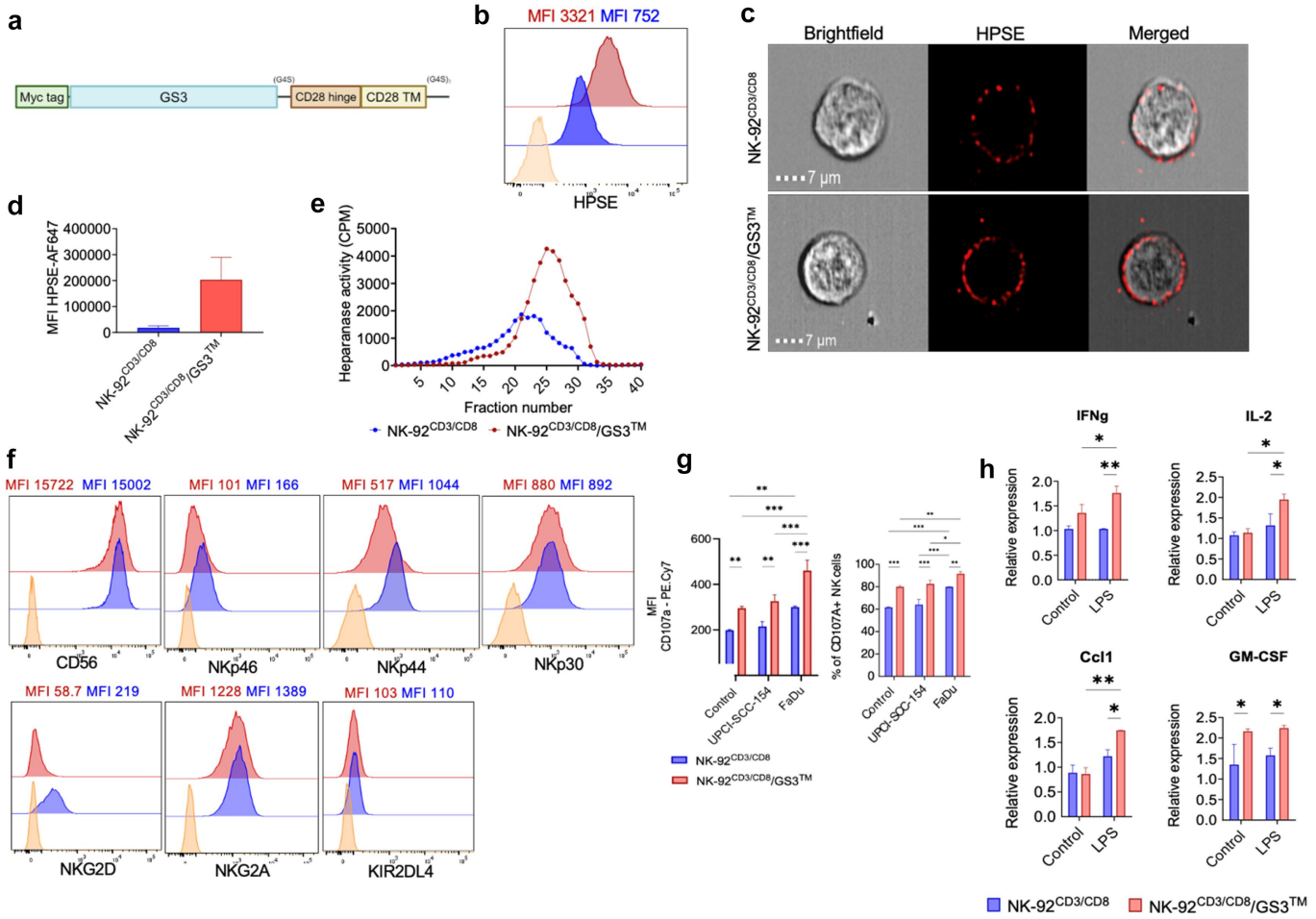


Figure 3. Construction and characterization of a cell line expressing the active form of HPSE on the plasma membrane (GS3^{TM}). (a) schematic representation of the GS3 fusion gene: [myc tag-GS3-CD28hinge-CD28TM (transmembrane domain)] used to generate the NK-92$^{CD3/CD8}$/GS3^{TM} cell line. (b) surface expression of endogenous HPSE and GS3 on NK-92$^{CD3/CD8}$/GS3^{TM} (red) and NK-92$^{CD3/CD8}$ (blue) cells labeled with anti-hpa 733 antibodies or isotype control (orange curve). The histogram displays the median fluorescence intensities (MFI) of three experimental replicates. (c) surface distribution of HPSE and GS3 on NK-92$^{CD3/CD8}$ and NK-92$^{CD3/CD8}$/GS3^{TM} cells stained with anti-hpa 733 antibodies (red fluorescence) analyzed by imaging flow cytometry. Representative pictures are shown. (d) quantification of HPSE/GS3. Results of two independent experiments are shown as the mean ± SD. (e) Representative results of two independent measurements of heparanase activity in NK cell lysates incubated for 18 hours on sulfate-labeled ECM as described elsewhere.[12] (f) flow cytometry profile of NK-92$^{CD3/CD8}$ and NK-92$^{CD3/CD8}$/GS3 for the indicated receptors. Histogram colors are as in (B). (g) activation of NK-92$^{CD3/CD8}$/GS3^{TM} and NK-92$^{CD3/CD8}$ cells co-incubated with the indicated HNSCC cell lines determined by CD107a detection. The MFI (left graph) and percentages (right graph) of CD107a^{+} degranulating cells are represented. (h) cytokine expression profile during resting state and upon stimulation of NK cells with lipopolysaccharide (LPS). cDNA was synthesized from total RNA and subjected to qPCR using primers specific for the indicated cytokines. Results are shown as the mean ± SD. Histograms are normalized to mode. Stars *, ** and *** represent p-values <0.05, <0.01 and <0.001, respectively.

with higher expression of NKG2D ligands (supplementary information, fig. S3). Furthermore, the expression of GS3^{TM} did not interfere with the induction of cytokine expression upon stimulation with LPS, which was higher in NK92$^{CD3/CD8}$/GS3^{TM} cells compared with non-transfected NK92$^{CD3/CD8}$ cells as measured by RT-qPCR (Figure 3h). Furthermore, this trend was confirmed by measuring IFN-γ secretion after treating the cells with LPS (supplementary information, fig. S4). Of note, primary feeder-cell-expanded NK cells showed also increased IFN-γ secretion upon LPS stimulation, albeit with significantly higher basal levels due to the presence of IL-2, which was present in the culture medium.

NK-92$^{CD3/CD8}$/GS3^{TM} cells show enhanced infiltration of tumor cell spheroids

Having confirmed the stable expression of active GS3^{TM} heparanase on the plasma membrane of NK-92$^{CD3/CD8}$/GS3^{TM} cells, we aimed at testing their infiltration through ECM in comparison with non-transfected cells. To this end, we performed a transmigration assay using transwell plates covered with Geltrex® matrix, a basement membrane extract that contains laminin, collagen IV, entactin, and heparan sulfate proteoglycans (supplementary information, Figure S5). In the lower chamber, medium containing the CCL19 ligand, which binds to the CCR7 chemokine receptor, acted as chemoattractant. After 24 hours of incubation the numbers of NK-92$^{CD3/CD8}$/GS3^{TM} cells measured in the lower chamber were significantly higher than those of non-transfected cells under the same conditions (Figure 4a), suggesting that GS3^{TM} facilitates the migration of the cells through the Geltrex® matrix.

We next examined the ability of the NK-92$^{CD3/CD8}$/GS3^{TM} cells to move in a 3-dimensional context. To this end, we prepared tumor spheroids of two different HNSCC cell lines: FaDu and PCI-13, both stably expressing mWasabi fluorescent protein. As shown in Figure 4b–e, confocal live microscopy experiments revealed significantly higher numbers of the NK-92$^{CD3/CD8}$/GS3^{TM} cells infiltrating the FaDu spheroids deep into the core, while the non-transfected NK-92$^{CD3/CD8}$ cells remained in the periphery of the spheroids under the same conditions. A similar experiment was performed with UPCI-SCC-154/mWasabi spheroids. We observed that after 12 h of co-culture, spheroids that were incubated with NK-92$^{CD3/CD8}$/

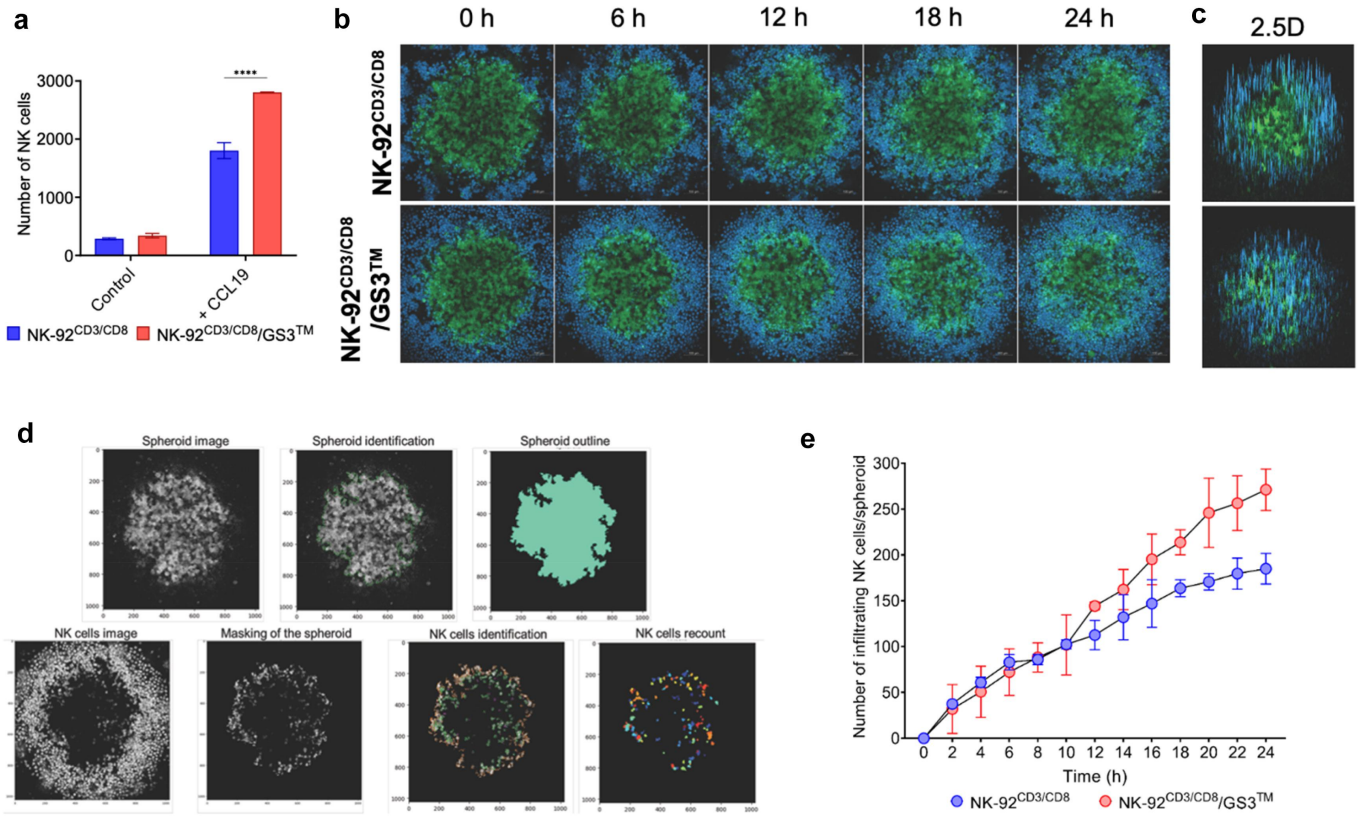


Figure 4. Transmigration assay and live microscopy analysis of co-cultures of NK-92$^{CD3/CD8}$/GS3^{TM} and NK-92$^{CD3/CD8}$ cells with tumor cell spheroids. (a) transwell migration assay comparing NK-92$^{CD3/CD8}$/GS3^{TM} and NK-92$^{CD3/CD8}$ cells. Matrigel was added to the upper inserts of the transwell plate and let to solidify for 18 h. Then, the cells were added on top of the Matrigel in X-Vivo20 medium, the lower chamber was filled with medium supplemented with CCL19 (300 ng/mL) or not (control). After 24 h, the cells in the lower chamber were collected and quantified by flow cytometry. (b) infiltration of NK-92$^{CD3/CD8}$GS3^{TM} cells into spheroids of FaDu cells generated in ultra-low attachment U-bottom plates for 48 h. Then, cocultures with either NK-92$^{CD3/CD8}$/GS3^{TM} or NK-92$^{CD3/CD8}$ cells were started and monitored for 24 h by confocal live cell imaging microscopy. Confocal images in the violet (NK-92 $^{CD3/CD8}$ cells) and green (FADU cells) channels were taken every hour for 24 h using a 5X magnification objective. Representative images are shown for the indicated time points. (c) Representative 2.5D images of the NK-92CD3/CD8 and NK-92CD3/CD8/GS3 cells generated with the ZEN image analysis software at 24 h f coculture. NK-92CD3/CD8/GS3 cells show higher degree of infiltration. (d) quantification of infiltrating NK cells using CellProfiler[20] as described elsewhere.[21] for the automatic image analysis, the spheroids were first identified using the image from the green channel (FADU cells), a mask of the spheroid was applied to the image in the blue channel (NK cells) and the numbers of NK cells within the spheroids were counted automatically for each image. (e) the number of infiltrating NK-92 cells quantified in (d) are plotted in a time-resolved manner expressed as mean ± sdev of three replicates.

GS3^{TM} had significantly lower size and higher NK cell infiltration (Supplementary Fig. S5E-F). These results verified the improved ability of the NK cells expressing GS3^{TM} to migrate through the compacted tumor cells in the spheroids.

Enhanced anti-tumor activity of NK-92$^{CD3/CD8}$ /GS3 cells in vivo

The encouraging results obtained in the transmigration and tumor spheroid experiments prompted us to test *in vivo* the ability of NK-92$^{CD3/CD8}$/GS3^{TM} cells to infiltrate tumor xenografts in immunodeficient mice in comparison with non-transfected cells. FaDu cells (5×10^6) were inoculated subcutaneously in the right flank of NOD-SCID mice, which after two weeks developed tumors of about 5 mm in diameter. Two groups of seven mice each then received either NK-92$^{CD3/CD8}$ or NK-92$^{CD3/CD8}$/GS3^{TM} cells injected i.v. at 4-day intervals (Figure 5a). External monitoring of tumor growth using a caliper showed statistically significant smaller tumors in mice receiving NK-92$^{CD3/CD8}$/GS3^{TM} cells. The day after the last injection, the mice were euthanized and the tumors resected for further analyses. At the end-point of the experiment, a significantly lower tumor weight was observed in mice inoculated with NK-92$^{CD3/CD8}$/GS3^{TM} cells compared with mice receiving NK-92$^{CD3/CD8}$ cells (mean 1.1 ± 0.2 g vs 1.71 ± 0.3 g; $p = 0.0030$) (Figure 5c). In both groups, the mice showed no signs of pathology throughout the duration of the treatment with the NK cells and the necropsy showed no evident signs of graft versus host pathology in any organs. We next analyzed the presence of NK-92$^{CD3/CD8}$/GS3^{TM} or non-transfected NK-92$^{CD3/CD8}$ cells in the tumors from the respective mice. NOD-SCID mice have impaired T and B cell lymphocyte development and, in the NOD background, they have defective NK cell function. Hence, no interference by the endogenous mouse NK cells as expected. We assessed the tumor-infiltrating NK-92 cells by quantitative RT-PCR of total RNA purified from the tumors using primers specific for CD56. As the mouse NK cells do not express CD56, this assay served to quantify just the NK-92$^{CD3/CD8}$/GS3^{TM} and NK-92$^{CD3/CD8}$ cells, which express comparable levels of CD56 (Figure 3f). Furthermore, we did a systematic analysis of CD56+ cells in serial sections of all the tumors using a Zeiss AxioScan.Z1 microscope, which

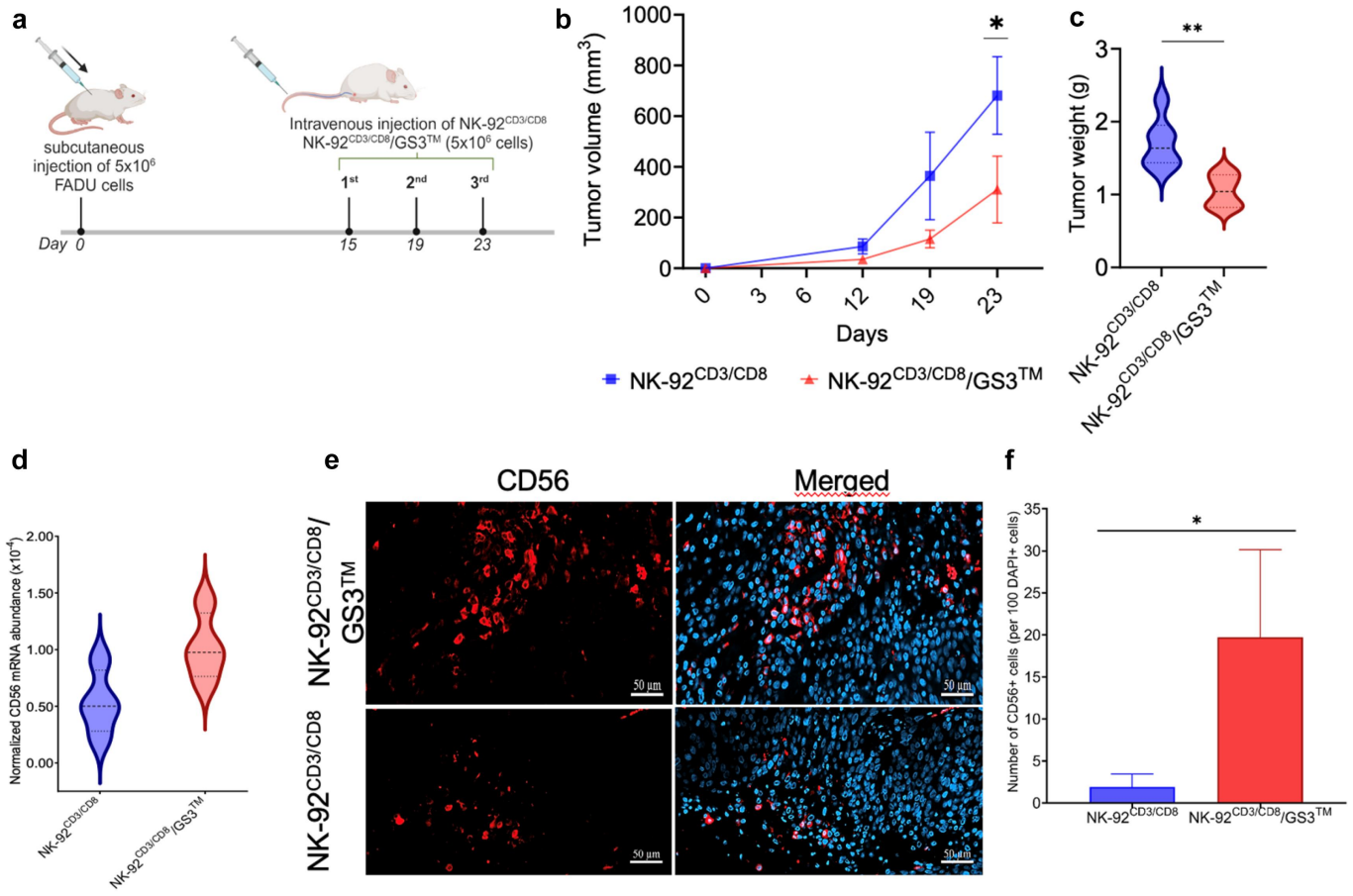


Figure 5. In vivo analysis of tumor infiltration by NK-92$^{CD3/CD8}$/GS3 cells. (a) experimental protocol of the xenograft mouse model. FaDu cells were implanted subcutaneously in the hind flank of SCID mice ($n = 21$). Monitorization was performed daily and when tumors reached 100–120 mm^3 the mice were randomized in three groups ($n = 7$): G1) NK-92$^{CD3/CD8}$ cells; G2) NK-92$^{CD3/CD8}$/GS3^{TM} cells; G3) vehicle (PBS). Injections (i.V.) were repeated at 4-day intervals. Three days after the last injection, tumors were excised, weighed and fixed in formalin for immunohistochemistry evaluation. A piece was taken for RNA extraction. (b) tumor volume measurements during the experiment shown as the mean ± SD. (c) tumor weight measured at the end of the experiment. Stars ** represent a p-value <0.01. (d) quantification of CD56 RNA from tumors by reverse transcription real time PCR, using specific primers for CD56 and GAPDH. (e) Representative microscopic images of 5-µm tumor sections from mice injected with NK-92CD3/CD8/GS3TM or NK-92CD3/CD8. Sections were stained with anti-human CD56 antibodies (red) and counterstained with DAPI (blue). (f) quantification of NK-92$^{CD3/CD8}$/GS3^{TM} or NK-92$^{CD3/CD8}$ infiltrating cells in tumor sections using CellProfiler™ software as described in methods. Three different microscopic fields (20X objective) were analyzed for the numbers of CD56+ cells detected in three different sections of each tumor. Note that, since mouse cells do not express CD56, only human NK-92$^{CD3/CD8}$/GS3^{TM} or NK-92$^{CD3/CD8}$ cells are detected with anti-CD56 antibodies. Data are mean values ± SD. (*) p-value = 0.0431.

automatically scans entire tissue sections. Significantly higher numbers of CD56+ cells were detected in tumors resected from mice that received NK-92$^{CD3/CD8}$/GS3^{TM} compared with those injected with NK-92$^{CD3/CD8}$ cells (Figure 5e).

Discussion

Solid tumors typically contain various types of immune cells, some activating (dendritic cells, NK and CD8 T cells) and some immunosuppressive (regulatory T cells, myeloid-derived suppressor cells, macrophages, neutrophils).[3] It is generally recognized that the presence of higher numbers of immune cells in a tumor correlates with longer overall survival of cancer patients.[4] Infiltration of tumor tissues by NK and T cells after extravasation requires controlled local degradation of ECM components, such as HSPGs, while HPSE is the only known endoglycosidase able to degrade HSPGs. Under physiological conditions, blood cells, in particular platelets, express high levels of HPSE, while its expression is low in solid tissues. Besides, cancer cells tend to overexpress HPSE,[7] which has been shown to support proliferative signaling and oncogenesis, inhibit apoptosis, induce angiogenesis, promote metastasis and evade anti-tumor immune responses.[15] Indeed, HPSE inhibitors,[22,23] such as polyanionic heparin-mimetics and covalent inhibitors based on pseudodisaccharides, have achieved tumor growth and metastasis reductions in preclinical studies in mice and some success in early clinical trials in cancer patients. However, to date no HPSE inhibitors have been approved for clinical use due to their off-tumor pleiotropic activity resulting in adverse effects, including a disability of immune cells to move through the TME.

To overcome the mechanisms used by cancer cells to evade the immune system, several lines of immunotherapies are being developed, which are mainly based on immune checkpoint inhibitors, TCR- or CAR-engineered T cells and NK cells. It is well established that higher frequencies of tumor infiltrating NK and CD8 T cells correlate with better prognosis. This implies that extravasation and mobility of these immune cells through solid tissues is a prerequisite for immune rejection of tumor cells. Previous studies have suggested that T cells loose HPSE expression when maintained *ex vivo* during genetic engineering for their use in ACT, and indicated that T cells engineered to overexpress HPSE had improved anti-tumor activity.[9] However, this strategy could have serious implications for tumor progression, since HPSE released by HPSE-overexpressing immune cells could support tumor cell mobility through the TME and hence metastasis.

In this study, measurements of HPSE on the surface of primary human NK cells upon activation either by co-culture with irradiated cancer cells or by treatment with a chemical activation cocktail, showed a transient increase in expression followed by a decay over time. Likewise, activated NK-92$^{CD3/CD8}$ cells showed a reduction in surface HPSE. However, in both cases the NK cells maintained a significant level of expression of surface HPSE. These results suggest that, as it has been pointed out for CD8 T cells, activated NK cells might have limited mobility through the ECM. In support of this hypothesis, our results with HPSE knock-out mice showed a substantial reduction in the infiltration capability of NK cells lacking HPSE. These observations granted an attempt to improve NK cell mobility by transfecting them to increase their expression of HPSE.

In the design of this study, we reasoned that genetically modifying NK cells to express an active form of HPSE (GS3) on the cell surface as an integral membrane protein (GS3^{TM}) could enhance their ability to infiltrate tumors without facilitating tumor development and metastasis. As immune cell model we used a derivative of the NK-92 cell line[24] that express constitutively the human CD3 and CD8 (NK-92$^{CD3/CD8}$),[21] which allows to perform expression and functional tests of both types of receptor TCR and CAR.[10] The antigen-independent tumor killing function of NK-92 cells is being subject of a number of clinical studies registered in Clinicaltrials.gov. We reasoned that if membrane-anchored HPSE could facilitate tumor infiltration of NK-92 cells, this strategy would be valid for primary NK cells as well as for CD8 T cells used for immunotherapy of solid tumors with different CAR and/or TCR T cell approaches. The GS3^{TM} protein was detected distributed throughout the cell surface with anti-myc and anti-Hpa 733 antibodies. The heparanase activity of the NK-92$^{CD3/CD8}$/GS3^{TM} cells was markedly higher compared with that of the parental non-transfected cell line. Interestingly, the surface expression of the NKp44, NKp46 and NKG2D receptors was diminished in NK-92$^{CD3/CD8}$/GS3^{TM} cells, yet their activation capabilities were preserved as demonstrated by the killing of tumor cells in the co-culture experiments.

The augmented heparanase activity of the NK-92$^{CD3/CD8}$/GS3^{TM} cells correlated with improved infiltration of ECM, as shown by the transmigration assay and the co-cultures with spheroids made of tumor cell lines. More importantly, the xenograft experiments with FaDu cells in mice showed reduced tumor growth in the mice treated with NK-92$^{CD3/CD8}$/GS3^{TM} cells, which correlated with higher numbers of CD56 infiltrating cells into the tumors. Taken together, our results demonstrate the suitability of GS3^{TM} to enhance the anti-tumor efficacy of effector immune cells.

Acknowledgments

This work was supported in part by the Cooperation Program in Cancer Research of the Deutsches Krebsforschungszentrum (DKFZ) and Israel's Ministry of Science, Technology and Space (MOST). IQ-F was supported by the University of Costa Rica and the German DAAD. SC-V was recipient of an Erasmus+ Intern Traineeship fellowship of the European Union. We thank Elisa Arias, Angela Diez and Kevin Delgado for technical assistance. We are grateful to the Flow Cytometry, Microscopy and Peptide Synthesis Core Facilities at DKFZ.

Disclosure statement

No potential conflict of interest was reported by the author(s).

Funding

The work was supported by the Cooperation Program in Cancer Research of the Deutsches Krebsforschungszentrum (DKFZ) and Israel's Ministry of Science, Technology and Space (MOST) [CA198].

ORCID

Angel Cid-Arregui http://orcid.org/0000-0003-1433-2922

Author contributions

IQF contributed to study design, conducted experimental work, data analysis, interpretation and representation, and wrote the manuscript. SLR, NI, LL RS, MB conducted experimental work, analyzed results, manuscript writing. IV project design, validation, writing review and editing. ACA conceived the idea, project design, experimental work, interpreted the results and wrote the manuscript. IQF, SLR, LL, S S, NI, SA, MM, IV and ACA verified the data. All authors had full access to all the data in the study and approved the final version of the manuscript.

Data availability statement

The data that support the findings of this study are available from the corresponding author, A C-A, upon reasonable request.

References

1. Peng L, Sferruzza G, Yang L, Zhou L, Chen S. Car-T and CAR-NK as cellular cancer immunotherapy for solid tumors. Cell Mol Immunol. 2024;21(10):1089–1108. doi:10.1038/s41423-024-01207-0.
2. Winstead E. FDA approves engineered cell therapy for advanced synovial sarcoma [official website of the United States government]. 2024 [updated 2024 Aug 27]. https://www.cancer.gov/news-events/cancer-currents-blog/2024/fda-tecelra-synovial-sarcoma-mage-a4.
3. de Visser KE, Joyce JA. The evolving tumor microenvironment: from cancer initiation to metastatic outgrowth. Cancer Cell. 2023;41(3):374–403.
4. Liu Y. Survival correlation of immune response in human cancers. Oncotarget. 2019;10(64):6885–6897. doi:10.18632/oncotarget.27360.
5. Laskowski TJ, Biederstadt A, Rezvani K. Natural killer cells in antitumour adoptive cell immunotherapy. Nat Rev Cancer. 2022;22(10):557–575. doi:10.1038/s41568-022-00491-0.
6. Cozar B, Greppi M, Carpentier S, Narni-Mancinelli E, Chiossone L, Vivier E. Tumor-infiltrating natural killer cells. Cancer Discov. 2021;11(1):34–44. doi:10.1158/2159-8290.CD-20-0655.
7. Vlodavsky I, Kayal Y, Hilwi M, Soboh S, Sanderson RD, Ilan N. Heparanase—A single protein with multiple enzymatic and nonenzymatic functions. Proteoglycan Res. 2023;1(3):e6. doi:10.1002/pgr2.6.
8. Nardella C, Lahm A, Pallaoro M, Brunetti M, Vannini A, Steinkuhler C. Mechanism of activation of human heparanase investigated by protein engineering. Biochemistry. 2004;43(7):1862–1873. doi:10.1021/bi030203a.
9. Caruana I, Savoldo B, Hoyos V, Weber G, Liu H, Kim ES, Ittmann MM, Marchetti D, Dotti G. Heparanase promotes tumor infiltration and antitumor activity of car-redirected T lymphocytes. Nat Med. 2015;21(5):524–529. doi:10.1038/nm.3833.
10. Poorebrahim M, Quiros-Fernandez I, Marme F, Burdach SE, Cid-Arregui A. A costimulatory chimeric antigen receptor targeting TROP2 enhances the cytotoxicity of NK cells expressing a T cell receptor reactive to human papillomavirus type 16 E7. Cancer Lett. 2023;566:216242. doi:10.1016/j.canlet.2023.216242.
11. Zcharia E, Jia J, Zhang X, Baraz L, Lindahl U, Peretz T, Vlodavsky I, Li J-P. Newly generated heparanase knock-out mice unravel co-regulation of heparanase and matrix metalloproteinases. PLOS ONE. 2009;4(4):e5181. doi:10.1371/journal.pone.0005181.
12. Zetser A, Levy-Adam F, Kaplan V, Gingis-Velitski S, Bashenko Y, Schubert S, Flugelman MY, Vlodavsky I, Ilan N. Processing and activation of latent heparanase occurs in lysosomes. J Cell Sci. 2004;117(11):2249–2258. doi:10.1242/jcs.01068.
13. Gutter-Kapon L, Alishekevitz D, Shaked Y, Li JP, Aronheim A, Ilan N, Vlodavsky I. Heparanase is required for activation and function of macrophages. Proc Natl Acad Sci USA. 2016;113(48):E7808–E17. doi:10.1073/pnas.1611380113.
14. Lin KY, Guarnieri FG, Staveley-O'Carroll KF, Levitsky HI, August JT, Pardoll DM, Wu TC. Treatment of established tumors with a novel vaccine that enhances major histocompatibility class II presentation of tumor antigen. Cancer Res. 1996;56(1):21–26.
15. Vlodavsky I, Ilan N, Sanderson RD. Forty years of basic and translational heparanase research. Adv Exp Med Biol. 2020;1221:3–59.
16. Vlodavsky I, Friedmann Y, Elkin M, Aingorn H, Atzmon R, Ishai-Michaeli R, Bitan M, Pappo O, Peretz T, Michal I, et al. Mammalian heparanase: gene cloning, expression and function in tumor progression and metastasis. Nat Med. 1999;5(7):793–802. doi:10.1038/10518.
17. Ai HW, Olenych SG, Wong P, Davidson MW, Campbell RE. Hue-shifted monomeric variants of clavularia cyan fluorescent protein: identification of the molecular determinants of color and applications in fluorescence imaging. BMC Biol. 2008;6(1):13. doi:10.1186/1741-7007-6-13.
18. Kowarz E, Loscher D, Marschalek R. Optimized sleeping beauty transposons rapidly generate stable transgenic cell lines. Biotechnol J. 2015;10(4):647–653. doi:10.1002/biot.201400821.
19. Mates L, Chuah MK, Belay E, Jerchow B, Manoj N, Acosta-Sanchez A, Grzela DP, Schmitt A, Becker K, Matrai J, et al. Molecular evolution of a novel hyperactive sleeping beauty transposase enables robust stable gene transfer in vertebrates. Nat Genet. 2009;41(6):753–761. doi:10.1038/ng.343.
20. Stirling DR, Swain-Bowden MJ, Lucas AM, Carpenter AE, Cimini BA, Goodman A. CellProfiler 4: improvements in speed, utility and usability. BMC Bioinf. 2021;22(1):433. doi:10.1186/s12859-021-04344-9.
21. Quiros-Fernandez I, Liborio-Ramos S, Leifert L, Schonfelder B, Vlodavsky I, Cid-Arregui A. Dual T cell receptor/chimeric antigen receptor engineered NK-92 cells targeting the HPV16 E6 oncoprotein and the tumor-associated antigen L1CAM exhibit enhanced cytotoxicity and specificity against tumor cells. J Med Virol. 2024;96(5):e29630. doi:10.1002/jmv.29630.
22. de Boer C, Armstrong Z, Lit VAJ, Barash U, Ruijgrok G, Boyango I, de Boer C, Weitzenberg MM, Schröder SP, Sarris AJC, et al. Mechanism-based heparanase inhibitors reduce cancer metastasis in vivo. Proc Natl Acad Sci USA. 2022;119(31):e2203167119. doi:10.1073/pnas.2203167119.
23. Mohan CD, Hari S, Preetham HD, Rangappa S, Barash U, Ilan N, Nayak SC, Gupta VK, Vlodavsky I, Rangappa KS, et al. Targeting heparanase in cancer: inhibition by synthetic, chemically modified, and natural compounds. iScience. 2019;15:360–390. doi:10.1016/j.isci.2019.04.034.
24. Klingemann H. The NK-92 cell line—30 years later: its impact on natural killer cell research and treatment of cancer. Cytotherapy. 2023;25(5):451–457. doi:10.1016/j.jcyt.2022.12.003.